
Molten iodide salt electrolyte for low-temperature low-cost sodium-based liquid metal battery

Qing Gong¹, Wenjin Ding^{1,*}, Alexander Bonk¹, Haomiao Li², Kangli Wang², Adrian Jianu³,
Alfons Weisenburger³, Andreas Bund⁴, Thomas Bauer⁵

¹Institute of Engineering Thermodynamics, German Aerospace Center (DLR), Stuttgart, Germany

²School of Electrical and Electronic Engineering, Huazhong University of Science and Technology (HUST), Wuhan, China

³Institute for Pulsed Power and Microwave Technology, Karlsruhe Institute of Technology (KIT),
Eggenstein-Leopoldshafen, Germany

⁴Electrochemistry and Electroplating Group, Technische Universität Ilmenau, Ilmenau, Germany

⁵Institute of Engineering Thermodynamics, German Aerospace Center (DLR), Cologne, Germany

*Corresponding author:

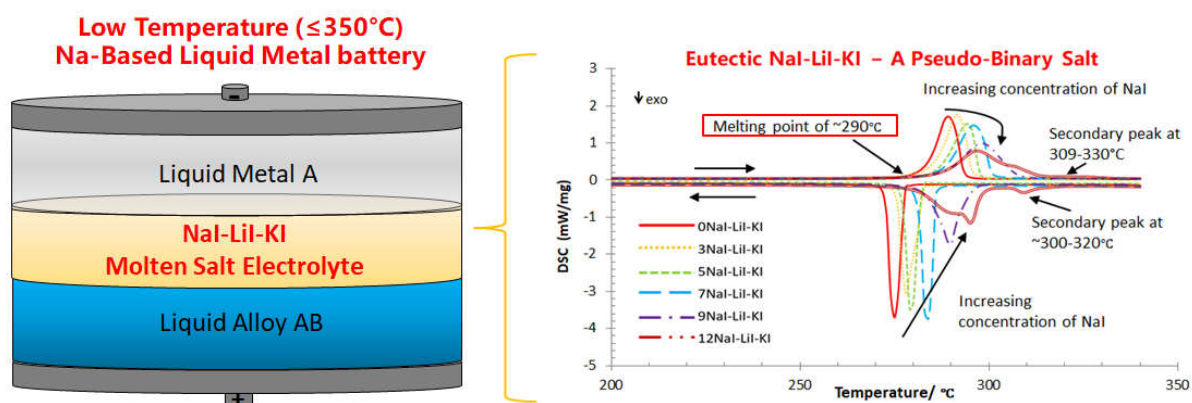
Tel.: +49 711 6862-233

Email: wenjin.ding@dlr.de

Abstract

Using low-melting-point electrolytes could overcome various key challenges of low-cost sodium-based liquid metal batteries (Na-LMBs), e.g. high rates of self-discharge and degradation of structural materials, by lowering their operation temperatures. Halide salts are considered promising electrolyte candidates for Na-LMBs due to their high stability and electrical conductivity. In this work, thermodynamic simulation via FactSageTM and thermal analysis via e.g., Differential Scanning Calorimeter (DSC), were carried out to explore the NaI-LiI-KI system, since it could be a promising electrolyte for Na-LMBs due to its low melting point and Na solubility. The results show that the eutectic NaI-LiI-KI performs as a pseudo-binary salt with a melting point of ~290 °C. In this pseudo-binary salt, the solubility of NaI in the eutectic LiI-KI is ~7 mol%. Using the eutectic NaI-LiI-KI electrolyte, Na-LMBs could be operated at < 350°C. Moreover, the Na solubility and Na⁺ conductivity of the eutectic NaI-LiI-KI, which are vital to the battery performance, were estimated based on the literature data via calculation. Additionally, the applicability and economic of NaI-LiI-KI were also discussed based on cost pre-analysis of salt materials, as well as of salt treatment and structural materials regarding salt corrosivity.

Graphical abstract



Highlights

- Eutectic NaI-LiI-KI is a promising low-melting-point electrolyte for Na-LMBs.
- Eutectic NaI-LiI-KI performs as a pseudo-binary salt with a melting point of $\sim 290^\circ\text{C}$.
- Solubility of NaI in the eutectic LiI-KI is ~ 7 mol% at $\sim 290^\circ\text{C}$.
- Na solubility and conductivity of Na^+ in NaI-LiI-KI are estimated by calculation.

Keywords: Differential scanning calorimeter (DSC), Grid-scale energy storage, Halide salt, Na solubility, Na^+ ionic conductivity, Pseudo-binary eutectic theory

1. Introduction

Given the continuously increasing share of renewable energy in the grid, large-scale stationary batteries play an essential role in grid-scale energy storage due to their small footprint and fast response [1]-[2]. As promising batteries for next generation grid-level storage power station, liquid metal batteries (LMBs) with three immiscible liquid layers have gained considerable attention in recent years owing to their excellent stability, high charge/discharge power level, low cost and simplicity for scaling-up [3]-[4]. Currently, several types of promising LMBs have been published, including Mg||Sb ($\text{MgCl}_2\text{--KCl--NaCl}$ electrolyte) [5], Ca-Mg||Bi (LiCl--CaCl_2 electrolyte) [6], Li||Pb-Sb (LiF--LiCl--LiI electrolyte) [7], Na||Bi (NaF--NaCl--NaI electrolyte) [3], Na||Pb-Bi (KCl--LiCl--NaCl electrolyte) [8], and Na||Zn (NaCl--CaCl_2 electrolyte) [10].

Sodium-based LMBs (Na-LMBs) have attracted extensive interest because sodium is a low cost and high earth-abundant element [3], [8]. Molten halide salts with high ionic conductivity ($> 1 \text{ S}\cdot\text{cm}^{-1}$) and high electrochemical/thermal stability ($> 2.5 \text{ V}$ for KI--LiI--NaI at $350\text{--}500^\circ\text{C}$) are mainstream electrolytes for LMBs [3]-[10]. Although researchers have investigated some other systems like molten NaOH--NaI [10-11] and room temperature ionic liquids (RTILs) [13]-[14] as low-temperature electrolytes for LMBs, the results were not satisfactory due to low electrochemical stability and/or low ionic conductivity. The molten halide salts have shown good performance in Li-LMB and Ca-LMB [6]-[7]. However, to our best knowledge, still no well performing halide salt electrolytes for low-temperature Na-LMBs (operation temperature $\leq 350^\circ\text{C}$) were published. Finding a molten salt electrolyte with low melting temperature, sufficient low solubility of sodium metal (i.e. low self-discharge rate) and ionic conductivity of Na^+ is the key issue for Na-LMBs.

The system LiCl--NaCl--KCl (Melting temperature $T_m \approx 350^\circ\text{C}$) has been used as an electrolyte for Na-LMBs due to its low melting point, low Na solubility, high stability and sufficient Na^+ conductivity. This salt system was selected to build Na-LMBs for fluid dynamic study at 450°C [8]. However, the performance of such batteries and electrolytes was not adequately explored. In the field of nuclear and rare earth industry, the eutectic LiCl--KCl is well known and was used as a low-melting-point and stable solvent to dissolve other chlorides, such as UCl_3 and LnCl_3 [15]-[17]. This $\text{MCl}_x\text{--}(\text{LiCl--KCl})_{\text{eut.}}$ ternary system was named a pseudo-binary system, in which a complete dissolution of the third chlorides MCl_x into $(\text{LiCl--KCl})_{\text{eut.}}$ leads to a little change of its melting point (generally $< 5^\circ\text{C}$) [15]-[17]. $\text{NaCl--}(\text{LiCl--KCl})_{\text{eut.}}$ with $< 10 \text{ mol\%}$ NaCl concentration is also included in such pseudo-binary system [15]-[17].

In order to find a lower melting point electrolyte ($T_m \leq 300^\circ\text{C}$) for low-temperature Na-based LMBs (operation temperature $\leq 350^\circ\text{C}$), it is worthwhile to investigate the system NaI-LiI-KI. Comparing with chlorine, iodine has lower electronegativity, thus theoretically the iodide salt has a lower melting point due to lower lattice energy between the iodine and metal ions [18]. As shown in Fig. 1 (estimated phase diagrams from FactSageTM, which have been validated via experimental data from literature), the phase diagram of the binary system LiI-KI is similar to LiCl-KCl, while the eutectic LiI-KI salt mixture has a lower melting point ($\sim 286^\circ\text{C}$) compared to the eutectic LiCl-KCl salt mixture ($\sim 353^\circ\text{C}$) [19]. Due to the similarity of these two halide salt systems, the NaI-(LiI-KI)_{eut.} ternary system is expected to also perform as a pseudo-binary system as NaCl-(LiCl-KCl)_{eut.} [20]. Thus, the NaI-LiI-KI system is expected to be a promising electrolyte for low-temperature ($< 350^\circ\text{C}$) Na-LMBs. However, to our best knowledge, very little data about NaI-LiI-KI, in particularly the experimental data, is available in literature due to strong hygroscopicity of iodide salts and thus high complexity of experiments. In 1991, Sangster and Pelton reported the simulated phase diagram of NaI-LiI-KI and pointed out there was no reported experimental data of this system at that time [20].

In this study, the NaI-(LiI-KI)_{eut.} system was investigated with thermodynamic simulation via FactSageTM and thermal analysis via Differential Scanning Calorimetry (DSC), Thermogravimetric-Mass Spectrometry (TG-MS) and a melting point apparatus (OptiMeltTM), in order to determine the melting points and salt compositions of the eutectic salt mixtures. Moreover, it was investigated if the NaI-LiI-KI system performs as a pseudo-binary eutectic system and shows the characteristic behavior of low melting point ($\leq 300^\circ\text{C}$) and high stability. Additionally, the Na solubility and conductivity of Na^+ in the molten NaI-LiI-KI, which are vital to the performance of Na-LMBs, were estimated via calculation based on the literature data of single salt [21]-[22].

2. Experimental

2.1. Sample preparation

Pure iodide salts including LiI (99% purity, dry, water $< 1.0\text{ wt\%}$, Alfa Aesar), NaI (99 % purity, dry, water $< 1.0\text{ wt\%}$, Alfa Aesar), KI (99 % purity, dry, water $< 1.0\text{ wt\%}$, Alfa Aesar) were used to synthesize the NaI-LiI-KI salt mixtures. Due to the strong hygroscopicity of iodide salts, the storage, weighing, mixing, and sample preparation of the salts were carried out in a glovebox (GS Glovebox System technik GmbH, Glovebox Mega 2, $\text{O}_2 < 0.5\text{ ppm}$, $\text{H}_2\text{O} < 10\text{ ppm}$) with ultra-high-purity argon gas (Ar 5.0, purity $> 99.999\%$). All salt mixtures ($\sim 5\text{ g}$) for thermal analysis were grinded in a ceramic mortar for at least 20 minutes by hand, so that they were mixed well with acceptable small salt particle size.

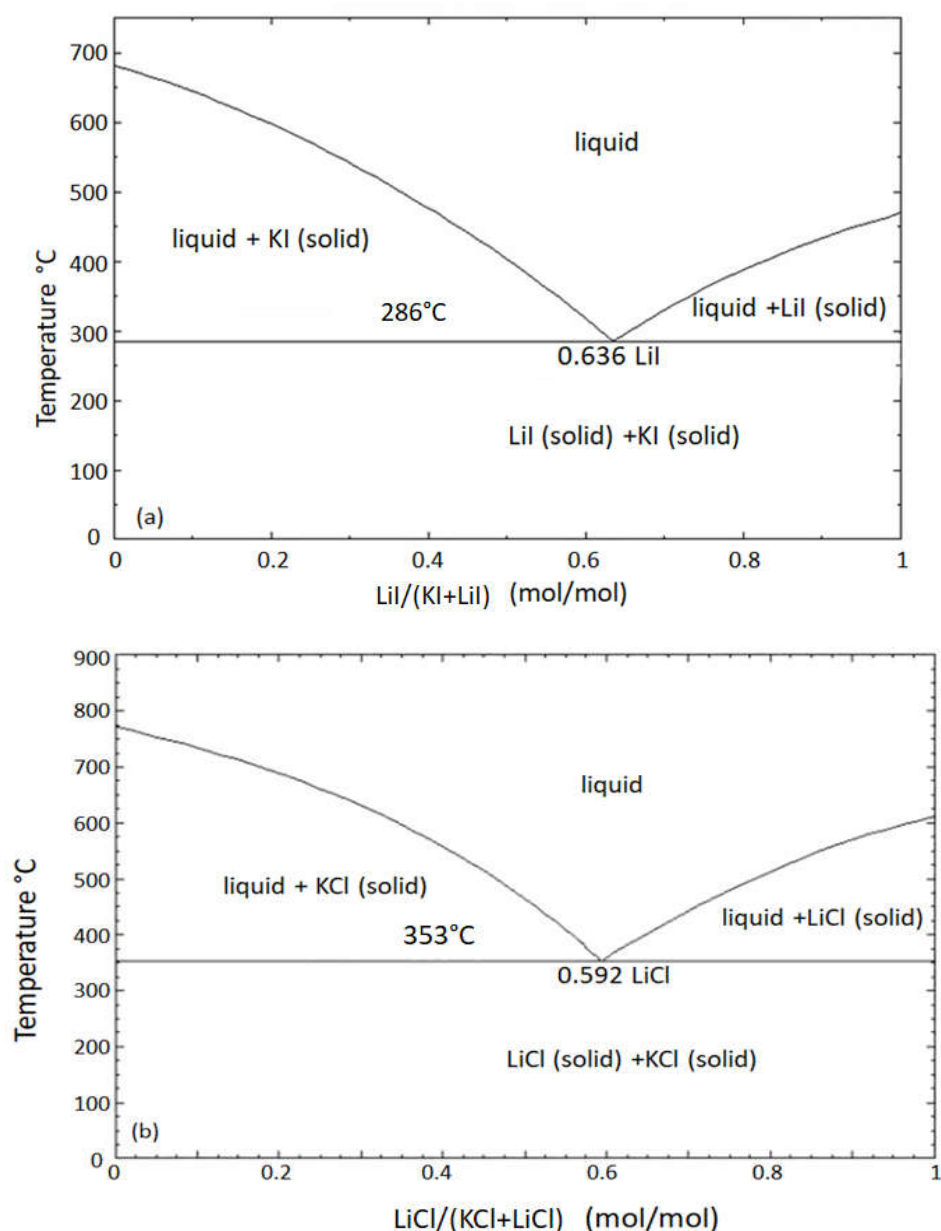


Fig. 1. Phase diagrams of the binary system (a) LiI-KI and (b) LiCl-KCl simulated with the commercial software package FactSage™.

2.2. Thermal analysis methods

2.2.1. Thermogravimetric mass spectrometry (TG-MS)

In order to study the effect of the salt hygroscopicity and dehydration on subsequent thermal analysis experiments, thermogravimetric mass spectrometry (TG-MS) experiments were carried out with a Simultaneous Thermo-Analysis device coupled with a Quadrupole Mass Spectrometer (STA 449C Jupiter® with QMS 403C Aëolos®, NETZSCH). The TG-MS

measurements on a selected salt mixture $9\text{NaI}-(\text{LiI-KI})_{\text{eut.}}$ sample were performed under argon flow (Ar 5.0, purity > 99.999 %, 20 ml/min). “ $x\text{NaI}-(\text{LiI-KI})_{\text{eut.}}$ sample” represents that x mol% NaI was added in the eutectic LiI-KI salt mixture, as shown in Table 1. 15 mg of the $9\text{NaI}-(\text{LiI-KI})_{\text{eut.}}$ sample was put into a platinum crucible and the crucible with salt was placed in a sealed glass bottle, which was taken out from glovebox. Then the crucible was transferred into the STA device with an exposure time in air about 2 minutes. The samples were firstly heated to 120 °C with rate of 10 K/min and kept at 120 °C for 30 min in order to release most of the weakly adsorbed water. After that, the sample was heated to 350 °C with rate of 10 K/min. The mass loss of the salt sample was recorded with TG device (i.e. STA device), while the released gases were analyzed with the MS device (i.e. QMS device) during the heating process.

2.2.2. Differential scanning calorimetry (DSC)

Differential Scanning Calorimetry (DSC) was used to determine melting points of iodides salt mixtures with different compositions. They were carried out with a commercial equipment of DSC 204 F1 Phoenix® (NETZSCH). The temperature calibration of the DSC equipment was conducted with standard materials (In, Sn, Zn, Bi, CsCl, Benzoic Acid, Biphenyl, KClO_4).

First, the aluminum lids of the aluminum crucibles were holed to prevent build-up of too high pressure in the crucibles during heating up. Subsequently, the crucibles with the lids were weighed and transferred into the glovebox. In the glovebox, about 10 mg of each tested iodide salt was charged into the crucible. Next, the crucible with the salt was sealed with the holed lid by a pressing with a toolkit in the glove box. Hereafter, all the produced samples were transferred out of the glovebox in sealed bottles with argon gas. Afterwards, the samples were weighed and put into the DSC equipment (exposure time in air about 2 minutes). The following parameters of DSC were set: Heating and cooling rates are 10 K/min, while protective gas flow around the furnace is N_2 (purity > 99.999%, Linde) at 20 ml/min. The reference crucible for the DSC measurement was an empty aluminum crucible.

Three cycles of DSC were performed for each salt sample. In the first cycle, in order to remove water from strongly hygroscopic iodine salts, a 10-minute isothermal heating was set at the temperature of 120°C according to the result of TG-MS experiments (see Section 3.2). Because a small amount of existing water was released from the samples and the salt samples became homogeneous by melting, the results of first cycle were not considered. For the second and third cycles, according to the estimated melting temperature of ~300°C, the investigated temperature range was between 150 and 350 °C. The results of second and

third cycles were compared among each other. The onset temperature of the melting peak in the second cycle was used to determine the melting temperature, as shown in Fig. 4 a).

2.2.3. Melting point measurement apparatus (OptiMelt™)

The Automated Melting Point System - OptiMelt™ (MPA 100, *Stanford Research Systems*) is a melting point measurement apparatus, which records with a camera the melting process of the salts in capillaries. The melting process of salts can be observed additionally with a magnifier window visually. For the purpose of observing the salt melting process and verifying with the results of DSC mutually, the experiments on the salt samples were carried out with OptiMelt™ in a glovebox.

Firstly, the capillary tubes were filled with the salt mixtures (up to 3 mm thick) and inserted in the OptiMelt™. The following parameters were set: the temperature range was 200-400 °C, heating rate of 10 K/min, which was consistent with the DSC experiments. For each experiment, two cycles were performed. In the first cycle, gas from the salts was exhausted to reduce bubbles in the molten salts for better observation. The images of second cycle from the built-in camera were used to determine the melting temperature of the studied salt sample. The temperature at which visual melting starts in the salt is defined as the melting temperature of the salt. Because the results were obtained from visual inspection, the accuracy of measured melting temperature is not as good as DSC. But OptiMelt experiments are still necessary supplement to research of melting point.

3. Results and discussion

3.1. Simulated phase diagram of NaI-LiI-KI

In order to find a suitable starting point for the study on the NaI-LiI-KI system, the module *Phase Diagram* of the commercial software FactSage™ based on the CALPHAD method was used to simulate the phase diagram of NaI-LiI-KI [23]. The simulated phase diagram in Fig. 2 shows that the ternary system NaI-LiI-KI shows no obviously eutectic points but a eutectic line representing pseudo-binary eutectic salt mixtures with an end on the eutectic point of LiI-KI. The points on the eutectic line have the melting temperatures of around 290 °C, close to the melting temperature of eutectic LiI-KI. This means that NaI is soluble in the eutectic LiI-KI salt mixture, and the solubility of NaI in the eutectic LiI-KI is found to be ~12 mol%. Using the analogy of the system NaI-LiI-KI to the NaCl-LiCl-KCl, it is therefore assumed in this work that NaI-LiI-KI is a pseudo-binary eutectic system.

In this work, the results from the simulated phase diagram were verified by experiments. Six points on the eutectic line in Fig. 2 were selected for experimental investigation with the

aforementioned thermal analysis methods. These six compositions of salts are summarized in Table 1. The ratio of Lil and KI is fixed at the eutectic composition (Lil:KI = 63.6:36.4 mol%) according to pseudo-binary eutectic theory, while the composition of NaI increases from 0 to 12 mol%.

Table 1. Six compositions of NaI-Lil-KI on the eutectic line in the simulated phase diagram selected for thermal analysis.

Samples	Lil (mol%)	KI (mol%)	NaI (mol%)
0NaI-(Lil-KI) _{eut.}	63.6	36.4	0
3NaI-(Lil-KI) _{eut.}	61.8	35.2	3
5NaI-(Lil-KI) _{eut.}	60.5	34.9	5
7NaI-(Lil-KI) _{eut.}	59.2	33.8	7
9NaI-(Lil-KI) _{eut.}	58	33	9
12NaI-(Lil-KI) _{eut.}	56.1	30.9	12

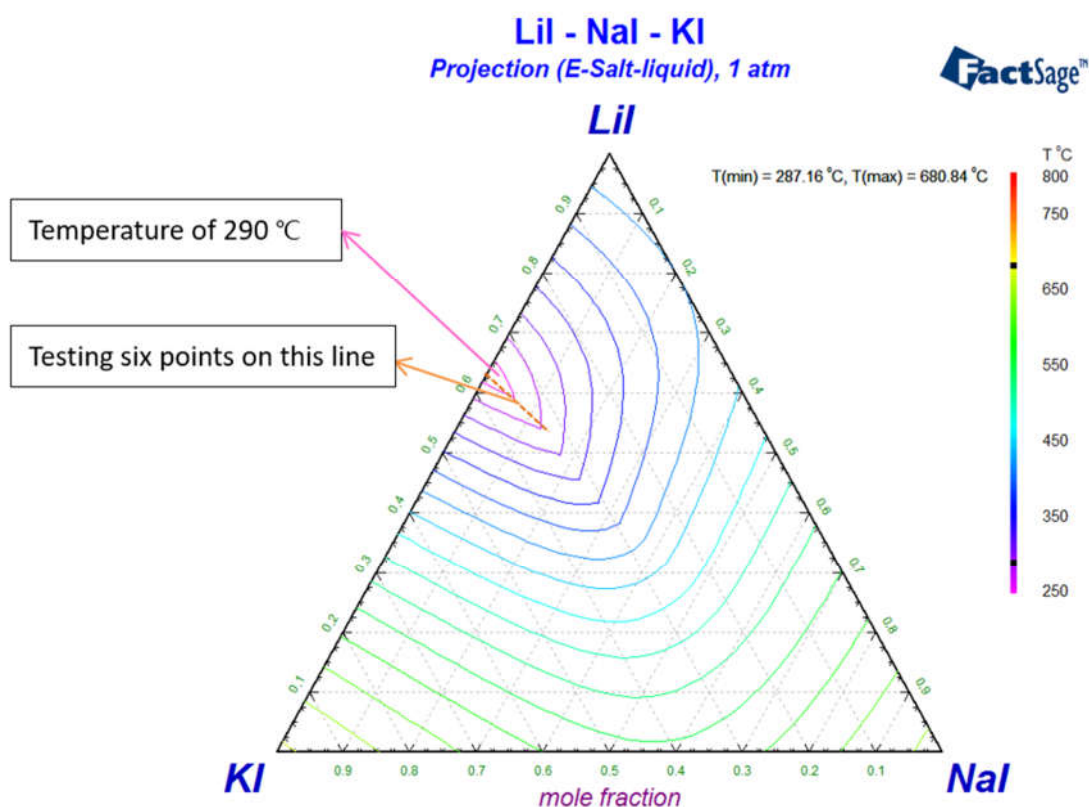


Fig. 2. Phase diagram of the liquidus line of the system NaI-Lil-KI simulated with the commercial software package FactSage™. Temperature gradient: 25°C.

3.2. TG-MS measurement

Fig. 3 shows the result of TG-MS for the salt mixture $9\text{NaI}-(\text{LiI-KI})_{\text{eut.}}$. In order to release the residual water, the sample was kept at $120\text{ }^{\circ}\text{C}$ for 30 minutes. According to the signal of H_2O (m/z 18 in Fig. 3), most of the residual water in the iodide salt was released after 10 minutes. In this stage, 1.06 wt% of mass loss was observed. The further mass loss up to the final temperature of $350\text{ }^{\circ}\text{C}$ was small, only 0.11 wt% of the total mass. In the whole experiment, no hydrolysis products such as HI (m/z 128) were detected with MS. The MS results show that the main mass loss was due to the release of residual water from the iodine salt. Moreover, no hydrolysis of the salt to HI and hydroxide species took place in this heating process. Thus, this heating process, i.e., a temperature held at 120°C for 10 min to release the residual water, was used for DSC measurements.

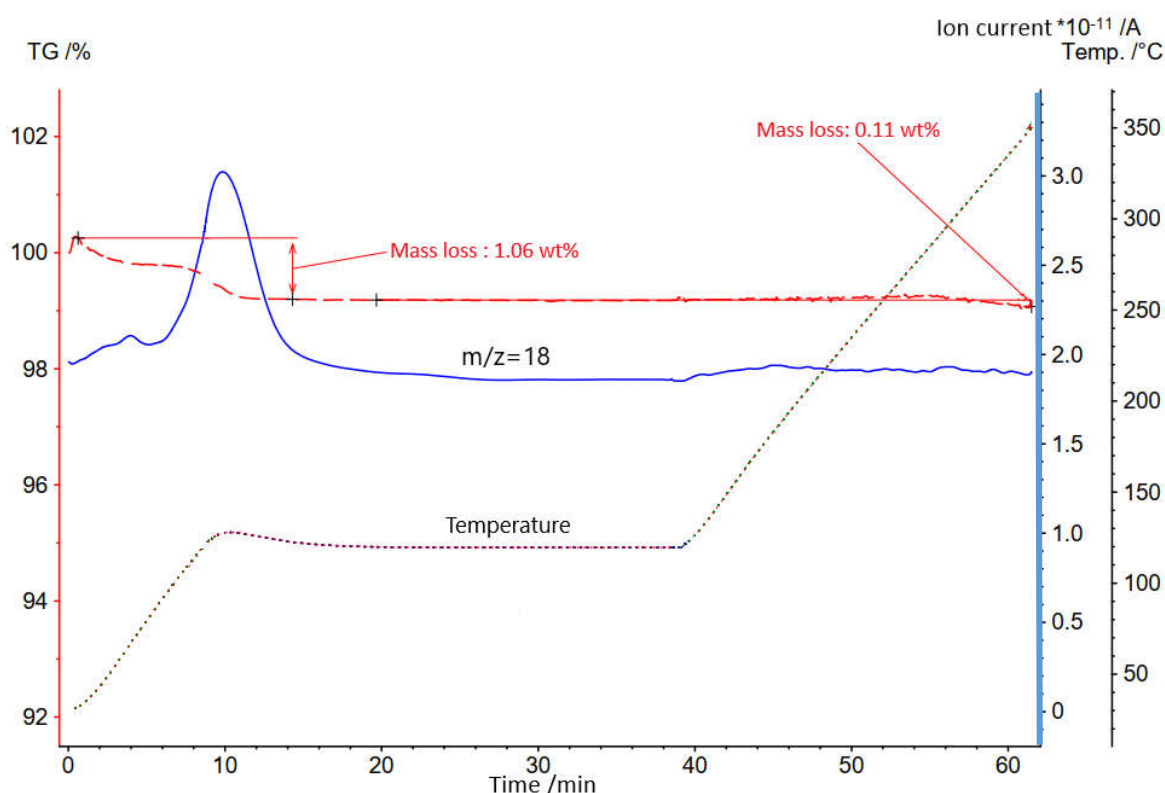


Fig. 3. TG-MS results of $9\text{NaI}-(\text{LiI-KI})_{\text{eut.}}$. $m/z=18$: signal of H_2O .

3.3. DSC measurements to determine melting point and eutectic compositions

The DSC measurements on the selected six salt mixtures shown in Table 1 show that the second and third heating cycles were almost identical. Therefore, for all the DSC curves shown in this work, the curves of the second cycles are presented. Fig. 4 a) shows the recorded important parameters for a studied salt sample (here $0\text{NaI}-(\text{LiI-KI})_{\text{eut.}}$), i.e., the

onset and end temperature of the melting peak and endset and end temperature of the crystallization peak. Among them, the onset temperature of the melting peak is used to determine the melting temperature of the salt. All essential DSC parameters of the studied samples are summarized in Table 2, while in Fig. 4 b) the DSC curves of the studied samples are shown in the same coordinate system for comparison.

As shown in Table 2 and Fig. 4 b), the influence of the NaI content on the melting behavior of $(\text{LiI-KI})_{\text{eut}}$ is evident. With the increasing concentration of NaI from 3 to 12 mol%, the width of the melting peak at 37% peak height increases from 7.5 to 17.2 °C. Generally, the non-eutectic salt mixtures $x\text{NaI}-(\text{LiI-KI})_{\text{eut}}$ have a wider melting peak, or a melting range, compared to the eutectic $(\text{LiI-KI})_{\text{eut}}$. Moreover, the onset temperature of the melting peak is also affected by the NaI content, which rises from 283.1 to 288.9 °C. Another noteworthy point is that when the concentration of NaI is 12 mol% obvious secondary peaks dissolution and crystallization of excess NaI (e.g., NaI, NaI-KI or NaI-LiI crystals) appear on the melting and crystallization curve, while for the concentration of NaI < 9 mol% no secondary peak at the temperature up to 350 °C can be observed. Additionally, comparing the onset temperature of melting with the endset temperature of crystallization, when the samples contain 7 mol% NaI, the onset temperature of melting (288.9 °C) is higher than the endset temperature of crystallization (286.0 °C), whereas when the sample contains 9 mol% NaI, the onset temperature of melting (288.8 °C) is lower than the endset temperature of crystallization (293.1 °C). This implies that the molten iodide salts with 9 mol% may be metastable (i.e., non-eutectic) in the temperature range from 288.8 °C to 293.1 °C. Thus, the solubility of NaI in the eutectic LiI-KI before formation of larger melting ranges is believed to be in the range of 7-9 mol%, which is lower than the estimated value from the FactSageTM simulation with a value of ~12 mol%.

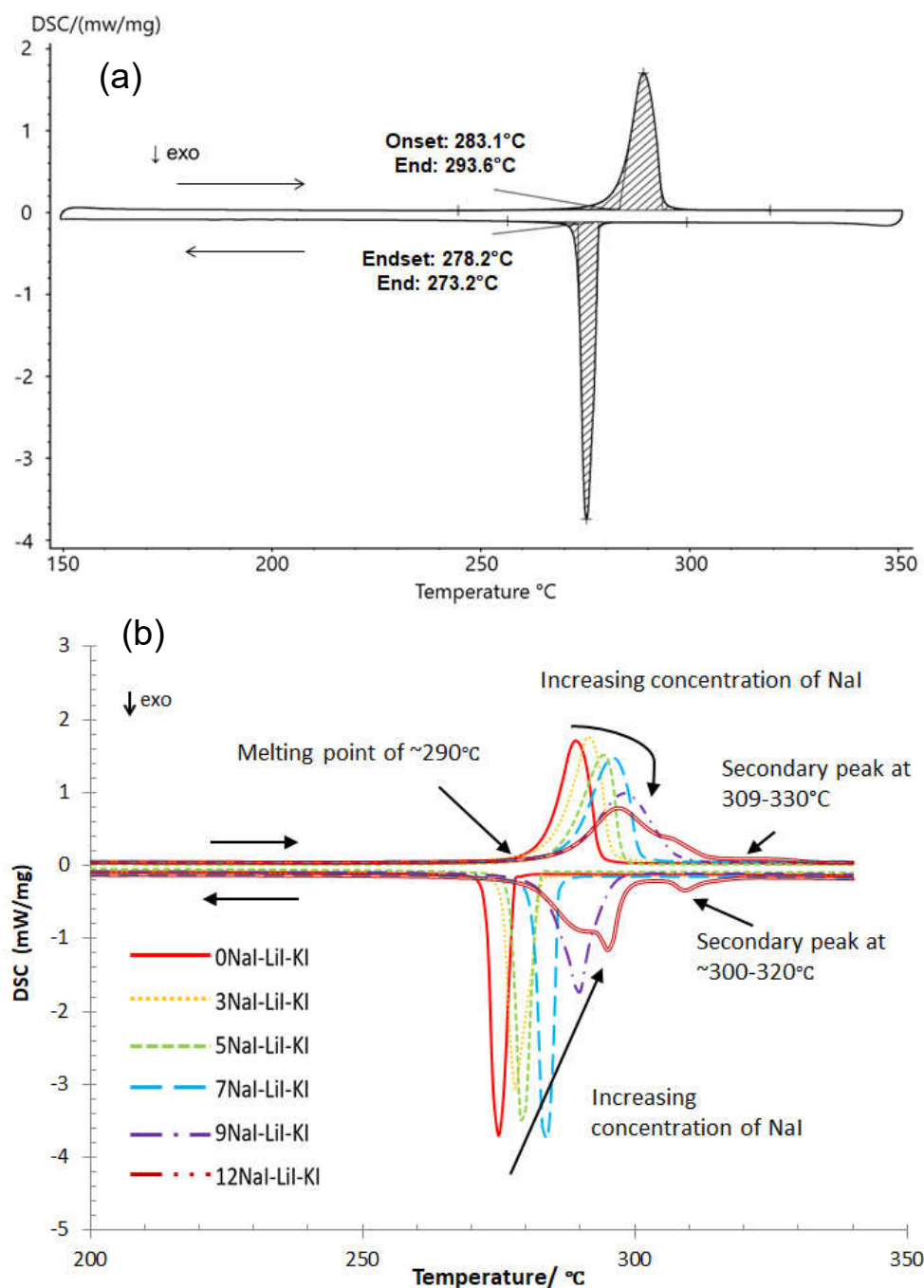


Fig. 4. DSC curves: (a) for 0NaI-(LiI-KI)_{eut.} with peak analysis showing the heating cycle at the top and the cooling cycle at the bottom, (b) for samples with increasing NaI concentration from 0 to 12 mol%. The DSC curves were tested for three cycles in the temperature range 150-350 °C and heating rate of 10 K/min. Only the second cycle in each DSC test is shown, as the curve of the first cycle contains water release and third cycle is almost identical. In (a), onset temperatures of melting and endset temperatures of crystallization in this work are the extrapolated onset and endset. The auxiliary line shows the drawing method of extrapolated onset and endset.

Table 2 Representative data from DSC curves of studied NaI-(LiI-KI)_{eut.} salts.

Samples	Onset temperature of main melting peak / °C	End temperature of main melting peak / °C	Width of melting peak at 37% peak height / °C	Endset temperature of main crystallization peak / °C	Secondary peak
0NaI-(LiI-KI) _{eut.}	283.1	293.6	7.8	278.2	No
3NaI-(LiI-KI) _{eut.}	285.6	295.4	7.5	282.9	No
5NaI-(LiI-KI) _{eut.}	286.5	297.5	8.1	282.1	No
7NaI-(LiI-KI) _{eut.}	288.9	300.6	9.2	286.0	No
9NaI-(LiI-KI) _{eut.}	288.8	306.9	13.4	293.1	No
12NaI-(LiI-KI) _{eut.}	287.6	312.3	17.2	298.7	Yes (heating:309- 330°C, cooling: 300-320°C)

3.4. Comparison of DSC and OptiMelt™ results

Fig. 5 presents the melting performance of NaI-LiI-KI with different NaI concentrations (0, 5 and 9 mol% as representatives) from 280 °C to 305 °C under the observation with OptiMelt™. As the results of DSC measurements, it is evident that the melting temperature increases with the increasing concentration of NaI. At 300 °C, the binary system without NaI melted completely, while there were some visible particles in the samples with 5 mol% and 9 mol% NaI. When the temperature increased to 305 °C, the melting of sample with 5 mol% NaI accomplished, whereas some particles were still observed in the 9NaI-(LiI-KI)_{eut.}. 9NaI-(LiI-KI)_{eut.} melted completely at the temperature of 330 °C. As shown in Table 3, the OptiMelt results (i.e., starting and end melting temperatures) agree well with the results of DSC (i.e., onset and end melting temperatures). The OptiMelt experiments confirmed the results of DSC that the solubility of NaI in the eutectic LiI-KI is considered to be in the range of 7-9 mol%. Moreover, the end melting temperature of 9NaI-(LiI-KI)_{eut.} obtained with OptiMelt™ is 23 °C higher than that from DSC. This confirms that 9NaI-(LiI-KI)_{eut.} is not completely pseudo-eutectic. The end melting temperature of 12NaI-(LiI-KI)_{eut.} from OptiMelt™ is ~340 °C, which is comparable to its end melting temperature obtained with DSC (i.e., end temperature of the secondary peak, 330 °C). Overall, although the results of OptiMelt experiments are not as accurate as DSC due to visual inspection, the results are well comparable to those of DSC. The (0-7)NaI-(LiI-KI)_{eut.} is believed to be eutectic and have the melting temperature below 300°C. The mixtures 3NaI-(LiI-KI)_{eut.}, 5NaI-(LiI-KI)_{eut.} and 7NaI-

(LiI-KI)_{eut.} are selected in the subsequent sections for Na solubility and Na⁺ conductivity calculations.

Table 3. Comparison of onset and end melting temperature from DSC and starting and end melting temperature from OptiMelt™.

Samples	Onset melting temperature (DSC) / °C	End melting temperature (DSC)* / °C	Starting melting temperature (OptiMelt) / °C	End melting temperature (OptiMelt) / °C
0NaI-(LiI-KI) _{eut.}	283.1	293.6	291	297
3NaI-(LiI-KI) _{eut.}	285.6	295.4	292	300
5NaI-(LiI-KI) _{eut.}	286.5	297.5	293	303
7NaI-(LiI-KI) _{eut.}	288.9	300.6	295	310
9NaI-(LiI-KI) _{eut.}	288.8	306.9	296	330
12NaI-(LiI-KI) _{eut.}	287.6	330	298	~340

*End melting temperature (DSC): the end temperature of main melting peak or secondary peak in the heating curve in Table 2.

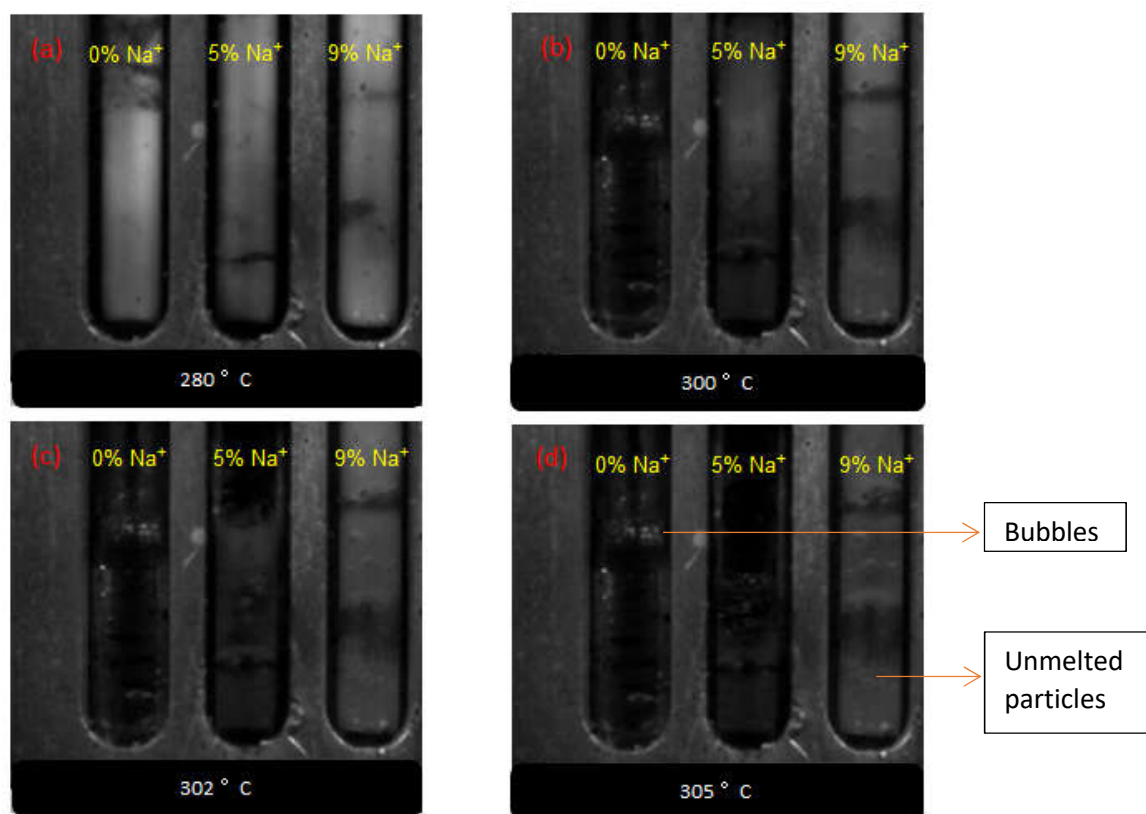


Fig. 5. OptiMelt™ results of LiI-KI-NaI system with fixed KI/LiI ratio of 63.6 : 36.4 mol%. The NaI concentrations of samples in capillary are 0 mol% (left), 5 mol% (center), and 9 mol% (right) respectively. Temperatures are 280 °C (a), 300 °C (b), 302 °C (c), and 305 °C (d). Heating rate: 10 K/min.

3.5. Estimation of Na solubility in NaI-LiI-KI

A low melting point electrolyte can not only reduce the operating temperature and manufacture difficulties (e.g. corrosion aspects, high Na vapor pressure, thermal design, sealings) of the LMBs [24], but also reduce their self-discharge rate by decreasing the solubility of Na in the electrolyte. Thus, the eutectic NaI-LiI-KI with low melting temperature < 300 °C is a promising electrolyte for Na-LMBs. However, to our best knowledge, the solubility of Na in NaI-LiI-KI (either experimental or simulation data) is not available in literature. In this work, the solubility of Na in the NaI-LiI-KI electrolyte is estimated via calculations based on the single salt data available in literature. For instance, the increase of the solubility of Na in NaI molten salt with increasing temperature [21] is shown in Fig. 6 a). It shows that the solubility of Na increases exponentially with temperature. Hence, the low operating temperature could restrain the solubility of Na in the electrolyte and reduce self-discharge of LMBs.

According to literature [22], the dissolution reaction of Na in Na⁺ containing molten halide salts (e.g., NaI and NaI-LiI-KI) occurs via Eq. 1:



This means that Na metal reacts with Na⁺ to form subvalent ions Na₂⁺ that dissolves in the melt. Thus, the equilibrium constant of this reaction can be given by the following equation [6], [22]:

$$K_{eq} = K_0 \exp\left(-\frac{\Delta_r G^\circ}{RT}\right) = a_{Na_2^+} / [a_{Na} \cdot a_{Na^+}], \quad \text{Eq. 2}$$

where K_0 is a constant, $\Delta_r G^\circ$ is the activation energy of this reaction, R the universal gas constant (8.314 J/(K·mol)), T the absolute temperature (K), $a_{Na_2^+}$, a_{Na} and a_{Na^+} is the activity of dissolved subvalent sodium ion (mol%), sodium metal in negative electrode ($a_{Na} = 1$ for pure Na), and sodium ion in the electrolyte (mol%), respectively.

From Eq. 2, the activity of dissolved subvalent sodium ($a_{Na_2^+}$) can be calculated from a_{Na^+} with:

$$a_{Na_2^+} = K_0 \exp\left(-\frac{\Delta_r G^\circ}{RT}\right) \cdot a_{Na^+}. \quad \text{Eq. 3}$$

When the ion concentration is low (e.g., <10 mol%), the ion activity can approximate with the concentration (i.e. activity coefficient is 1). Thus, the solubility of Na metal is related to the concentration of Na⁺ in the melt according to Eq. 4.

$$c_{Na_2^+} \approx K_0 \exp\left(-\frac{\Delta_r G^\circ}{RT}\right) \cdot c_{Na^+}. \quad \text{Eq. 4}$$

Under the assumption that the activation energy of Na dissolution in Na⁺ containing molten iodide salts (pure NaI or NaI-LiI-KI) is the same, the solubility of Na in the xNaI-(LiI-KI)_{eut} could be estimated at different temperatures using Eq. 4. In order to obtain linear relationship, Eq. 4 is transformed to:

$$\ln c_{Na_2^+} = \ln K_0 + \ln c_{Na^+} - \left(\frac{\Delta_r G^\circ}{R}\right) \cdot \frac{1}{T}. \quad \text{Eq. 5}$$

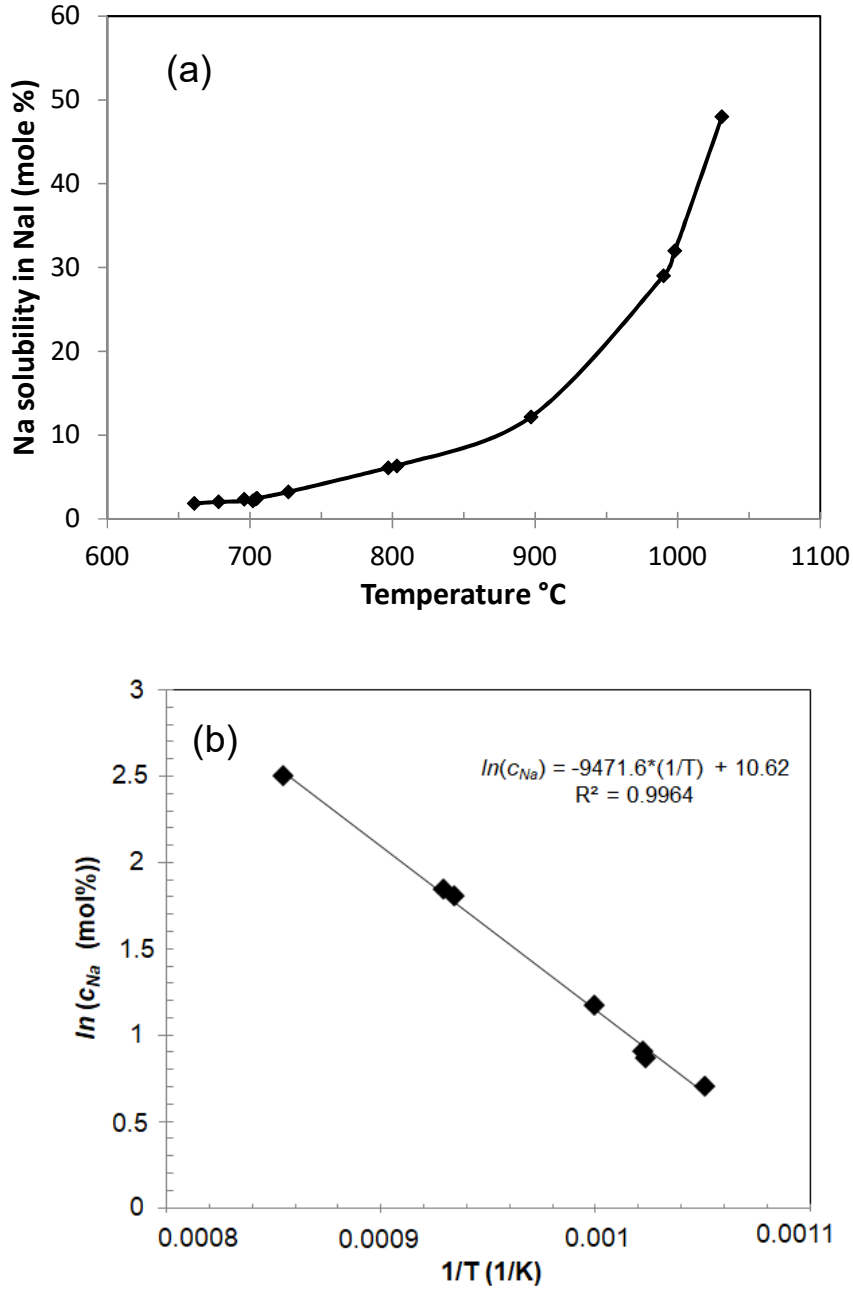


Fig. 6. (a) Temperature dependence of Na solubility $c_{Na_2^+}$ in pure NaI [21] and (b) Fitted curve of $\ln c_{Na_2^+}$ vs. $\frac{1}{T}$ for determination of activation energy of Na dissolution reaction.

Using the data (NaI: 2-12 mol%) in Fig. 6 a), the linear relationship of $\ln c_{Na_2^+}$ and $\frac{1}{T}$ for pure molten NaI is obtained with the least-squares method and shown in Fig. 6 b). The activation energy of Na dissolution reaction ($\Delta_r G^\circ$) is estimated to be ~ 78.7 kJ/mol ($9471.6 \times 8.314 / 1000 = 78.7$ kJ/mol, $R^2 = 0.9964$). Using this activation energy, the solubility of Na in pure NaI salt is estimated to be ~ 0.5 mol% at 657 °C, which is comparable to the value (1.6 mol% at 657 °C) in [3]. Fig. 7 shows that using the same activation energy and Eq. 5 the estimated solubilities of Na in (3-7)NaI-(LiI-KI)_{eut} are below 0.03 mol% at < 550 °C. It is

lower than that of Li in LiCl (> 0.5 mol% at 640 °C) or LiI (> 1 mol% at 468 °C) [3]. Based on Eq. 4, this may be explained with not only low melting temperature (T) but also low Na^+ concentration (c_{Na^+}). However, the Na solubilities of Na in NaI-(LiI-KI)_{eut} may be underestimated using the method presented in this work, if Na metal can react with other cations (i.e., Li^+ , K^+) to form subvalent ions NaLi^+ and NaK^+ that dissolves in the melt. To our knowledge, such experimental data or theory is less in literature. Our future work will investigate this with e.g., the experimental measurements of Na solubilities in pure LiI and KI.

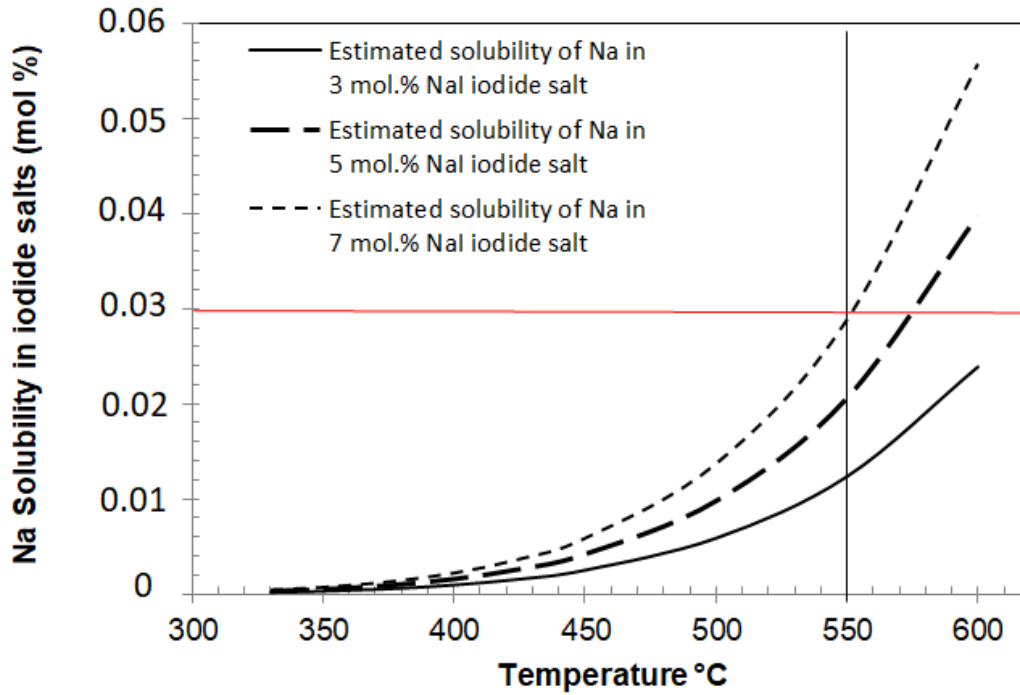


Fig. 7. Estimated solubility of Na in NaI-LiI-KI salts with 3-7 mol% NaI at the temperature of 330 °C to 600 °C.

3.6. Estimation of Na^+ conductivity in NaI-LiI-KI

The effective conductivity (i.e. sodium-ionic conductivity) of the electrolyte is another crucial parameter for battery performance. For the sake of low anode solubility and low operating temperature, the concentration of NaI in NaI-LiI-KI system should be limited (< 9 mol%, see previous sections), which may lead to insufficient Na^+ conductivity of the electrolyte for the Na-LMBs.

To our best knowledge, there is lack of experimental investigation and less available literature data on effective conductivity of the molten salt electrolyte for LMBs. In this work, in order to estimate the effective conductivity of NaI-LiI-KI for Na-LMBs, the following hypotheses are suggested:

- (1) The Na⁺ ions are the only effective ions for conductivity,
- (2) The Na⁺ conductivity relates linearly to the concentration of Na⁺ ions, according to Kohlrausch's law for independent migration of ions [25],
- (3) The total conductivity of NaI-LiI-KI is represented by the conductivity of pure NaI available in literature [26], since the conductivity of the NaI-LiI-KI ternary system is not yet available, and the conductivities of NaI, LiI and KI are in the same order of magnitude due to their similarity [26].

Thus, the effective conductivity of NaI-LiI-KI with different Na⁺ concentrations can be estimated using Eq. 8:

$$\kappa_{eff} = \kappa_{total} \times c_{Na^+} \approx \kappa_{pure\ NaI} \times c_{Na^+}, \quad \text{Eq. 8}$$

where the temperature dependence of the conductivity of pure NaI is given by Eq. 9 in S/cm [26]:

$$\kappa_{pure\ NaI} = -2.8948 + 7.5861 \times 10^{-3}T - 2.2381 \times 10^{-6}T^2. \quad \text{Eq. 9}$$

As shown in Fig. 8, the estimated effective conductivities of NaI-LiI-KI with 3-7 mol% NaI are higher than 28 mS/cm for T>350°C. This value is higher than that of LiPF₆ in EC/DMC (50:50 wt%) as the electrolyte of conventional lithium ion battery (~10.48 mS/cm) [27], but lower than that of 37 wt% H₂SO₄ as the electrolyte of lead-acid battery (~742 mS/cm) at room temperature [28]. The experimental results on the Na-based LMBs with NaCl-LiCl-KCl electrolytes in [8] show that when the electrolyte contained only 9 mol% NaCl, the battery did not show obvious internal resistance at 450 °C, i.e., the effective conductivity of such electrolyte was sufficient. To determine the optimal concentration of NaI in NaI-LiI-KI regarding Na solubility and effective conductivity, experimental investigation with Na solubility measurements and Na-LMBs cell test is suggested as future work.

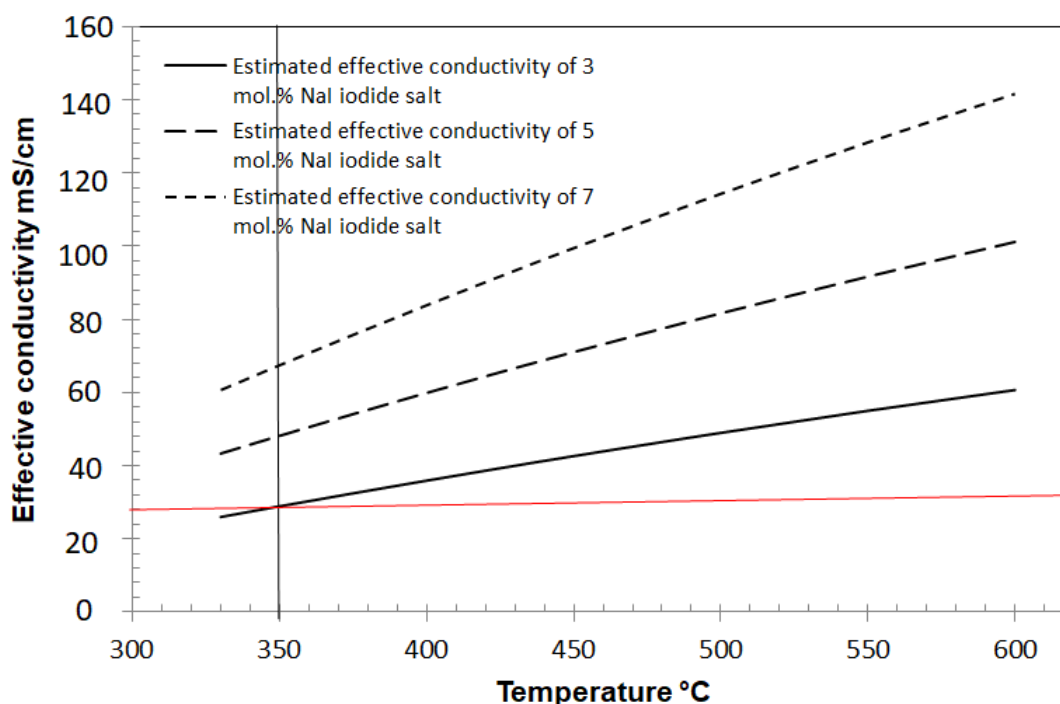


Fig. 8. Estimated effective conductivity of NaI-LiI-KI with 3-7 mol% NaI at 330-600 °C.

3.7. Cost analysis of NaI-LiI-KI as molten salt electrolyte for Na-LMB

The eutectic NaI-LiI-KI system has been shown a promising low-temperature electrolyte for Na-LMBs regarding its low melting temperature, estimated low Na solubility and sufficient Na^+ conductivity. In this subsection, its applicability and economic is discussed based on cost analysis of salt materials, salt treatment and structural materials.

Based on the current large-scale prices of single iodide salts (see Generally, strong corrosivity of molten halogen salts to the metallic structural materials is the main challenge for realizing their high-temperature applications, e.g., as thermal energy storage materials in concentrated solar power plants, as heat transfer fluids in molten salt nuclear plants [29]. The corrosion behavior of structural materials, mainly commercial metallic alloys, in contact with e.g. molten halogen salts at high temperatures has been extensively investigated [30]-[32]. In theory, the pure halogen salts cannot oxidize the metal elements in the commercial Cr-Fe-Ni alloys, when they are thermodynamically more stable than Fe-, Cr- and Ni-halogen salts [31]. This means that the pure NaI-LiI-KI salt mixture is not corrosive to the commercial Cr-Fe-Ni alloys. However, the iodide salts are strongly hygroscopic and can be hydrated in a short contact with air. If such salt is not properly treated during the melting process, the hydrated water in the salt can react with the iodide salts to form some corrosive impurities, mainly the hydroxyl species and HI. Such molten salt can be very corrosive to the metallic structural materials, particularly at high temperatures [30]. In order to allow using affordable

alloys such as stainless steels for a long lifetime of the battery (> 20 years), the salt should be treated to reduce its corrosivity, e.g., by salt purification [33] or adding corrosion inhibitors like Mg metal [29]. In Section 3.2, a simple heating process for the NaI-LiI-KI salt mixture is suggested by the TG-MS measurements to release the most water for reducing its corrosivity. Moreover, since the LMBs generally work under an inert atmosphere and the Na metal can inhibit corrosion by reducing the redox potential of the molten iodide salts, the corrosivity against the metallic structural materials is not a critical issue for the NaI-LiI-KI salt mixture as a molten salt electrolyte in the Na-LMB. The similar or same salt treatment and structural materials for other common electrolytes can be used for the NaI-LiI-KI electrolyte. Overall, the NaI-LiI-KI electrolyte is applicable for Na-LMBs after the cost analysis of salt materials, salt treatment and structural materials.

Table 4), the materials costs of the eutectic NaI-LiI-KI salt mixture are calculated ~20 USD/kg, higher than other molten salt electrolytes (e.g., NaCl-LiCl-KCl ~3 USD/kg, NaF-NaCl-NaI ~2 USD/kg) for Na-LMBs. However, regarding that only a thin molten salt electrolyte (generally ~ 1 cm thick) is required, the materials costs of Na-LMBs are mainly defined by the electrode costs [3]. Thus, the use of the NaI-LiI-KI (or NaCl-LiCl-KCl) electrolyte will not lead to a significant cost increase of Na-LMBs compared to other electrolytes, even when the prices of Li salts increase significantly due to large-scale use of Li-ion batteries in E-cars.

Generally, strong corrosivity of molten halogen salts to the metallic structural materials is the main challenge for realizing their high-temperature applications, e.g., as thermal energy storage materials in concentrated solar power plants, as heat transfer fluids in molten salt nuclear plants [29]. The corrosion behavior of structural materials, mainly commercial metallic alloys, in contact with e.g. molten halogen salts at high temperatures has been extensively investigated [30]-[32]. In theory, the pure halogen salts cannot oxidize the metal elements in the commercial Cr-Fe-Ni alloys, when they are thermodynamically more stable than Fe-, Cr- and Ni-halogen salts [31]. This means that the pure NaI-LiI-KI salt mixture is not corrosive to the commercial Cr-Fe-Ni alloys. However, the iodide salts are strongly hygroscopic and can be hydrated in a short contact with air. If such salt is not properly treated during the melting process, the hydrated water in the salt can react with the iodide salts to form some corrosive impurities, mainly the hydroxyl species and HI. Such molten salt can be very corrosive to the metallic structural materials, particularly at high temperatures [30]. In order to allow using affordable alloys such as stainless steels for a long lifetime of the battery (> 20 years), the salt should be treated to reduce its corrosivity, e.g., by salt purification [33] or adding corrosion inhibitors like Mg metal [29]. In Section 3.2, a simple heating process for the NaI-LiI-KI salt mixture is suggested by the TG-MS measurements to release the most water for reducing its corrosivity. Moreover, since the LMBs generally work

under an inert atmosphere and the Na metal can inhibit corrosion by reducing the redox potential of the molten iodide salts, the corrosivity against the metallic structural materials is not a critical issue for the NaI-LiI-KI salt mixture as a molten salt electrolyte in the Na-LMB. The similar or same salt treatment and structural materials for other common electrolytes can be used for the NaI-LiI-KI electrolyte. Overall, the NaI-LiI-KI electrolyte is applicable for Na-LMBs after the cost analysis of salt materials, salt treatment and structural materials.

Table 4. Large-scale prices of single salts and eutectic salt mixture of NaI-LiI-KI system.

Salts	Large-scale prices / USD/kg	Sources
NaI	~3	Current price (CP)*
KI	~4	CP
LiI	~40	CP
NaI-LiI-KI eutectic	~20	Calculated with CPs of single salts
NaCl-LiCl-KCl eutectic	~3	Calculated with CPs of single salts
NaF-NaCl-NaI eutectic	~2	Calculated with CPs of single salts

*CP: current large-scale price of the single salt from www.alibaba.com [Accessed on May 9th of 2020].

4. Conclusions

In this work, thermodynamic simulation of the phase diagram and thermal analysis methods were used to investigate the NaI-LiI-KI system as a low-temperature electrolyte for Na-LMBs. The results show that it can be considered as a pseudo-binary eutectic molten salt system. The eutectic NaI-LiI-KI system has a melting point of ~290 °C, while the solubility of NaI in the eutectic LiI-KI molten salt is ~7-9 mol%. Thus, with this electrolyte, the operation temperature of Na-LMBs can be reduced to $\leq 350^{\circ}\text{C}$. Such a low operating temperature helps to overcome the key challenges of Na-LMBs, e.g., high rates of self-discharge, material corrosion, high Na vapor pressure. The Na solubility and Na^+ conductivity in the molten NaI-LiI-KI, which are vital to the battery performance, were estimated based on the literature data. The estimated Na solubility in $\text{NaI-(LiI-KI)}_{\text{eut.}}$ with 7 mol% NaI is lower than 0.03 mol% at $< 550^{\circ}\text{C}$, while the estimated effective conductivities are higher than 28 mS/cm at $T > 350^{\circ}\text{C}$. Thus, the operation temperature in a range from 350 °C to 550 °C seems feasible. To determine the optimal concentration of NaI in NaI-LiI-KI regarding Na solubility and effective conductivity, experimental investigation with Na solubility measurements and Na-LMBs cell test is suggested as future work.

In summary, the NaI-LiI-KI salt mixture is a promising candidate as electrolyte for Na-LMBs, because it meets the following demands: 1) As halide molten salts, it has high electrochemical stability and ionic conductivity; 2) The melting temperature of NaI-LiI-KI is

the lowest among all published halide salt electrolytes for LMB, which can help reduce operation temperature and self-discharge of Na-LMBs.

Acknowledge

This research has been performed within the DFG-NSFC Sino-German project (DFG Project Number 411450529): 'Study on Corrosion Control and Low-Temperature Electrolytes for Low-Cost Na-based Liquid Metal Batteries', which is funded by Deutsche Forschungsgemeinschaft (DFG) and National Natural Science Foundation of China (NSFC). The authors would like to thank their colleagues Dr. Carolina Villada, Markus Braun and Andrea Hanke at the DLR-Institute of Engineering Thermodynamics for their support.

Reference

- [1] Z. Yang, J. Zhang, M.C. Kintner-Meyer, X. Lu, D. Choi, J.P. Lemmon and J. Liu, Electrochemical energy storage for green grid, *Chem. Rev.*, 111 (2011) 3577-3613. <https://pubs.acs.org/doi/abs/10.1021/cr100290v>.
- [2] B. Dunn, H. Kamath and J.-M. Tarascon, Electrical energy storage for the grid: a battery of choices, *Science*, 334 (2011) 928-935. <https://doi.org/10.1126/science.1212741>.
- [3] H. Kim, D.A. Boysen, J.M. Newhouse, B.L. Spatocco, B. Chung, P.J. Burke, D.J. Bradwell, K. Jiang, A.A. Tomaszowska and K. Wang, Liquid metal batteries: past, present, and future, *Chem. Rev.*, 113 (2013) 2075-2099. <https://doi.org/10.1021/cr300205k>.
- [4] H. Li, H. Yin, K. Wang, S. Cheng, K. Jiang and D.R. Sadoway, Liquid metal electrodes for energy storage batteries, *Advanced Energy Materials*, 6 (2016) 1600483 <https://doi.org/10.1002/aenm.201600483>.
- [5] D.J. Bradwell, H. Kim, A.H. Sirk and D.R. Sadoway, Magnesium–antimony liquid metal battery for stationary energy storage, *Journal of the American Chemical Society*, 134 (2012) 1895-1897 <https://doi.org/10.1021/ja209759s>.
- [6] T. Ouchi, H. Kim, B.L. Spatocco and D.R. Sadoway, Calcium-based multi-element chemistry for grid-scale electrochemical energy storage, *Nature communications*, 7 (2016) 1-5 <https://doi.org/10.1038/ncomms10999>.
- [7] K. Wang, K. Jiang, B. Chung, T. Ouchi, P.J. Burke, D.A. Boysen, D.J. Bradwell, H. Kim, U. Muecke and D.R. Sadoway, Lithium–antimony–lead liquid metal battery for grid-level energy storage, *Nature*, 514 (2014) 348-350 <https://doi.org/10.1038/nature13700>.
- [8] T. Weier, A. Bund, W. El-Mofid, G. Horstmann, C. Lalau, S. Landgraf, M. Nimtz, M. Starace, F. Stefani and N. Weber, Liquid metal batteries-materials selection and fluid dynamics, in: *IOP Conference Series: Materials Science and Engineering*, 228 (2017) 012-013. <https://doi.org/10.1088/1757-899X/228/1/012013>.
- [9] W.J. Hamer, M.S. Malmberg, B. Rubin, Theoretical electromotive forces for cells containing a single solid or molten fluoride, bromide, or iodide, *J. Electrochem. Soc.* 112 (1965) 750-755. <https://doi.org/10.1149/1.2423683>.
- [10] J. Xu, O.S. Kjos, K.S. Osen, A.M. Martinez, O.E. Kongstein and G.M. Haarberg, Na-Zn liquid metal battery, *Journal of Power Sources*, 332 (2016) 274-280. <https://doi.org/10.1016/j.jpowsour.2016.09.125>.
- [11] R.F. Ashour, H. Yin, T. Ouchi, D.H. Kelley and D.R. Sadoway, Communication—molten amide-hydroxide-iodide electrolyte for a low-temperature sodium-based liquid metal battery, *Journal of The Electrochemical Society*, 164 (2017) A535-A537. <https://doi.org/10.1149/2.1451702jes>.

-
- [12] B.L. Spatocco, T. Ouchi, G. Lambotte, P.J. Burke and D.R. Sadoway, Low-temperature molten salt electrolytes for membrane-free sodium metal batteries, *Journal of The Electrochemical Society*, 162 (2015) A2729-A2736. <https://doi.org/10.1149/2.0441514jes>.
- [13] C.C. Lalau, A. Dimitrova, M. Himmerlich, A. Ispas, T. Weier, S. Krischok and A. Bund, An electrochemical and photoelectron spectroscopy study of a low temperature liquid metal battery based on an ionic liquid electrolyte, *Journal of The Electrochemical Society*, 163 (2016) A2488-A2493. <https://doi.org/10.1149/2.0051613jes>.
- [14] C.C. Lalau, A. Ispas, T. Weier and A. Bund, Sodium-bismuth-lead low temperature liquid metal battery, *J. Electrochem. Plating Technol.*, JEPT-4808 (2015). <https://doi.org/10.12850/ISSN2196-0267.JEPT4808>.
- [15] K. Nakamura and M. Kurata, Thermal analysis of pseudo-binary system: LiCl-KCl eutectic and lanthanide trichloride, *Journal of nuclear materials*, 247 (1997) 309-314. [https://doi.org/10.1016/S0022-3115\(97\)00099-8](https://doi.org/10.1016/S0022-3115(97)00099-8).
- [16] S. Ghosh, R. Ganesan, R. Sridharan and T. Gnanasekaran, Investigation on the Phase Diagram of LiCl-KCl-NdCl₃ Pseudo-Ternary System, *Journal of Phase Equilibria and Diffusion*, 39 (2018) 916-932. <https://doi.org/10.1007/s11669-018-0695-3>.
- [17] K. Sridharan, T. Allen, M. Anderson and M. Simpson, Thermal properties of LiCl-KCl molten salt for nuclear waste separation, Univ. of Wisconsin, Madison, WI (United States), 2012. <https://doi.org/10.2172/1058922>.
- [18] J. Huheey, E. Keiter, R. Keiter, *Anorganische Chemie: Prinzipien von Struktur und Reaktivität*, Walter de Gruyter GmbH & Co KG, 2014 (in German).
- [19] FactSage FTSalt - FACT Salt Phase Diagrams (338), 23 March 2020, http://www.crct.polymtl.ca/fact/documentation/FTSalt/FTSalt_Figs.htm.
- [20] J. Songster and A.D. Pelton, Thermodynamic calculation of phase diagrams of the 60 common-ion ternary systems containing cations Li, Na, K, Rb, Cs and anions F, Cl, Br, I, *Journal of phase equilibria*, 12 (1991) 511-537. <https://doi.org/10.1007/BF02645064>.
- [21] M. Bredig and H. Bronstein, Miscibility of liquid metals with salts. IV. The sodium-sodium halide systems at high temperatures, *The Journal of Physical Chemistry*, 64 (1960) 64-67. <https://doi.org/10.1021/j100830a016>.
- [22] M. Bredig, *Mixtures of metals with molten salts*, Oak Ridge National Lab., Tenn, 1963
- [23] C.W. Bale, E. Bélisle, P. Chartrand, S.A. Decterov, G. Eriksson, K. Hack, I.H. Jung, Y.B. Kang, J. Melançon, A.D. Pelton, C. Robelin, and S. Petersen, FactSage thermochemical software and databases—recent developments, *Calphad*, 33.2 (2009) 295-311. <https://doi.org/10.1016/j.calphad.2008.09.009>.
- [24] J. Kim, D. Shin, Y. Jung, S.M. Hwang, T. Song, et al., LiCl-LiI molten salt electrolyte with bismuth-lead positive electrode for liquid metal battery, *Journal of Power Sources*, 377 (2018) 87-92. <https://doi.org/10.1016/j.jpowsour.2017.11.081>
- [25] G. Castellan, *Physical Chemistry*. Ed, Addison-Wesley Publishing Company, New York, 1983.
- [26] *Molten salts: Volume 1. Electrical conductance, density, and viscosity data*, 1968.
- [27] P. Porion, Y. R. Dougassa, C. Tessier, L. El. Ouatani, J. Jacquemin, and M. Anouti, Comparative study on transport properties for LiFAP and LiPF₆ in alkyl-carbonates as electrolytes through conductivity, viscosity and NMR self-diffusion measurements, *Electrochimica Acta*, 114 (2013) 95-104. <https://doi.org/10.1016/j.electacta.2013.10.015>.
- [28] H.E. Darling, Conductivity of Sulfuric Acid Solutions, *Journal of Chemical & Engineering Data*, 9.3 (1964): 421-426. <https://doi.org/10.1021/jc60022a041>.
- [29] W. Ding, H. Shi, A. Jianu, Y. Xiu, A. Bonk, et al., Molten chloride salts for high-temperature thermal energy storage: Mitigation strategies against corrosion of structural materials. *Sol. Energ. Mater. Sol. Cells*, 193 (2019) 298-313. <https://doi.org/10.1016/j.solmat.2018.12.020>.

-
- [30] W. Ding, H. Shi, Y. Xiu, A. Bonk, A. Weisenburger et al., Hot corrosion behavior of commercial alloys in thermal energy storage material of molten $\text{MgCl}_2/\text{KCl}/\text{NaCl}$ under inert atmosphere. *Sol. Energy Mater. Sol. Cells*, 184 (2018) 22–30. <https://doi.org/10.1016/j.solmat.2018.04.025>.
- [31] W. Ding, A. Bonk, T. Bauer, Corrosion behavior of metallic alloys in molten chloride salts for thermal energy storage in concentrated solar power plants - A review. *Front. Chem. Sci. Eng.*, 12(3) (2018) 564-576. <https://doi.org/10.1007/s11705-018-1720-0>
- [32] N.S. Patel, V. Pavik, M. Boca, High-temperature corrosion behavior of superalloys in molten salts – A review. *Critical Review in Solid State and Materials Sciences*, 42(1) (2017) 83-97. <https://doi.org/10.1080/10408436.2016.1243090>
- [33] J.M. Kurley, P.W. Halstenberg, A. McAlister, S. Raiman, S. Dai, et al., Enabling chloride salts for thermal energy storage: implications of salt purity. *RSC Adv.*, 9 (2019) 25602-25608. <https://doi.org/10.1039/C9RA03133B>